

## Window Optical Microstructures (Review)

V. A. Maiorov\*

Novgorod State University, Veliky Novgorod, 173003 Russia

\* e-mail: Vitaly.Maiorov@novsu.ru

Received April 8, 2020; revised April 8, 2020; accepted May 4, 2020

**Abstract**—The results of research on the development and application of optical elements placed in the upper part of the window in order to redirect sunlight to the ceiling and into the interior of the room have been summarized and analyzed. There has been a steady trend of transferring such devices to the micro level. The article has described the structures and optical characteristics of three types of the optical microstructures embedded in double-glazed windows: microprismatic films, panels with prismatic microstructures on two sides, and films with embedded micro-mirrors. It has been noted that the use of curved surfaces instead of flat ones in microstructures improves the optical properties and increases the uniformity of the redirected sunlight flux. The designs and properties of optical microelectromechanical systems: switchable micro-mirrors and micro-blinds that were manufactured using microelectronics technology, have been generalized.

**Keywords:** windows, optical microstructures, sunlight redirection

**DOI:** 10.1134/S0030400X20100185

### INTRODUCTION

Side natural lighting through windows in the walls is the main way of lighting public and residential premises.

Standard windows have significant disadvantages.

1. In direct sunlight, the illumination is excessively high at the window, quickly decreases as you move away from it, and is insufficient in the interior of the room.

2. The window does not eliminate the glare. The glare is a visual condition with excessive brightness or a high uneven distribution of brightness in the field of view.

The idea of a complex design of a side window, formed by the beginning of the XXI century, offers a way to eliminate these shortcomings [1]. The complex window consists of two parts (Fig. 1).

1. The upper part, which is the part of natural light, redirects sunlight to the ceiling and into the depth of the room. Its lower edge is located above the eyes of the person standing in the room (1.8 m), which allows you to avoid getting redirected light into the eyes.

2. The lower part, which is the viewing part, provides a visual contact with the environment (viewing outside) and also eliminates glare on the work surface near the window.

By the beginning of the XXI century, three types of the optical elements placed in the upper part of the window were proposed for redirecting sunlight: prismatic panels, laser-cut panels, and LUMITOP® devices that redirect sunlight [1]. These devices have

a number of disadvantages because of their significant weight and dimensions. Since the beginning of the XXI century, continuous research and development has been carried out to improve the window optical devices. The main direction of this research is to reduce their size: the miniaturization with the transition to the micro level.

Reducing the size of optical structures does not change the optical properties and avoids deviations from the laws of geometric optics (diffraction) until their dimensions reach the visible light wavelength range. Optical microstructures are defined as surface structures with transverse and longitudinal dimensions of the order of 10–1000  $\mu\text{m}$ . Moving optical structures to the micro level makes it easier to embed

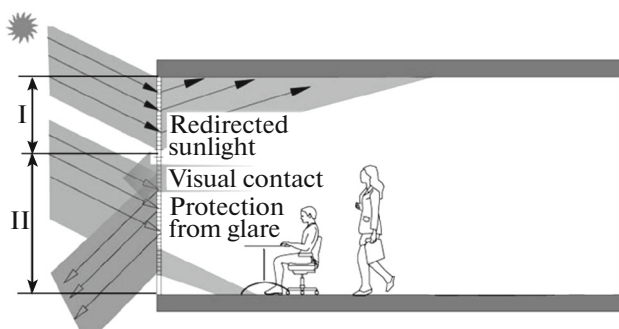


**Fig. 1.** A complex window with various functions of the upper I and lower II parts.

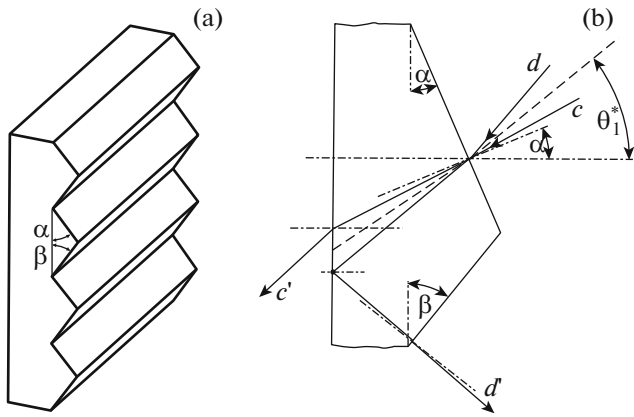


**Fig. 2.** (a) A panel with a three-sided prismatic structure and (b) the direction of sun beams ( $c-c'$ ) passing through the panel and ( $d-d'$ ) reflected by it [2].

them in windows and reduces the visual impact they cause.

This paper presents an analysis of research carried out over the past 20 years on the development and application of window optical microstructures. The main direction of the development is to miniaturize existing optical devices, so it is logical to follow the trend of changing the properties of optical devices as their size decreases. These microstructures are used to redirect sunlight and are placed at the top of the window.

## 1. PRISMATIC MICROSTRUCTURES

### 1.1. Prismatic Panels

The prismatic panels for redirecting sunlight to the depth of the room were already proposed to be used in the early XX century. However, the complexity of manufacturing such glass products and the coming era of artificial electric lighting buried this technology. The energy crisis of the 1970s and the availability of polymethylmethacrylate (PMMA) caused the second birth of prismatic panels at the end of the XX century. A detailed analysis of the research performed on the calculation and use of three-sided prismatic panels in natural lighting devices is performed in [2].

A prismatic panel is a plate with horizontal prismatic edges (Fig. 2). The properties of a three-sided prismatic panel are determined by the  $\alpha$  and  $\beta$  angles of the slope of the faces. Sunlight is refracted on the prism surface and changes direction. The maximum angle of inclination to the horizon  $\theta_1^*$  separates the solar rays passing through the panel ( $c-c'$ ) from the rays ( $d-d'$ ) that are reflected from it because of full internal reflection at the back surface.

Prismatic panels are made of PMMA by molding. The finished product is installed in a sealed double-

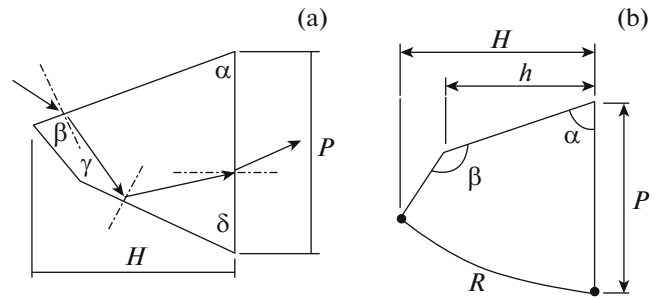


**Fig. 3.** The shape and main geometric characteristics of four-sided microprisms: (a) type 1 with flat faces and (b) type 2 with one curved face, modified [6].

glazed window. The prismatic panels are used for two purposes:

- (i) they are placed in lamps on the roofs to protect from direct sunlight;
- (ii) they are installed in the windows to change the direction of sunlight.

The angles of the faces are determined based on the location of the panel. When installing a double-glazed window with prismatic panels in overhead lights, a mirror reflecting coating is applied to one of the faces of the prism by vacuum spraying of aluminum [3]. You can achieve the necessary ratio between the shares of passing and reflected light by selecting the angles of inclination of the prismatic panel faces.

The German company Siteco Beleuchtungstechnik GmbH occupies a leading position in the production of three-sided prismatic panels for natural lighting systems [3]. The cost of prismatic panels (without double-glazed windows) is about 200 €/m<sup>2</sup>.

### 1.2. Microprismatic Films

Microprismatic film was first developed by a group of researchers in Taiwan in 2010 [4–6]. There are two types of microprismatic structure (Fig. 3). The structure of the type 1 has a four-sided shape with a profile height of  $H = 50 \mu\text{m}$ , a pitch of  $P = 50 \mu\text{m}$ , and  $\alpha = 45^\circ$ . A modified structure of the type 2 has a curved face. The prism is four-sided, two heights  $H = 21.2 \mu\text{m}$  and  $h = 20 \mu\text{m}$ , pitch  $P = 18 \mu\text{m}$ , radius of curvature of the curved face  $R = 32.3 \mu\text{m}$ , and angles  $\alpha = 69^\circ$  and  $\beta = 151^\circ$ .

A curved face evenly scatters a parallel beam of light into a widely diverging beam because of full internal reflection. Moreover, scattering occurs when the angle of inclination  $\theta_1$  of the incident solar radiation changes significantly (Fig. 4).

Figure 5 shows the indicatrix of the scattering of the sunlight incident at the angle to the horizon  $\theta_1 = 40^\circ$  for microprismatic structures of both types. A sweep of these scattering indicatrices is shown in Fig. 6.

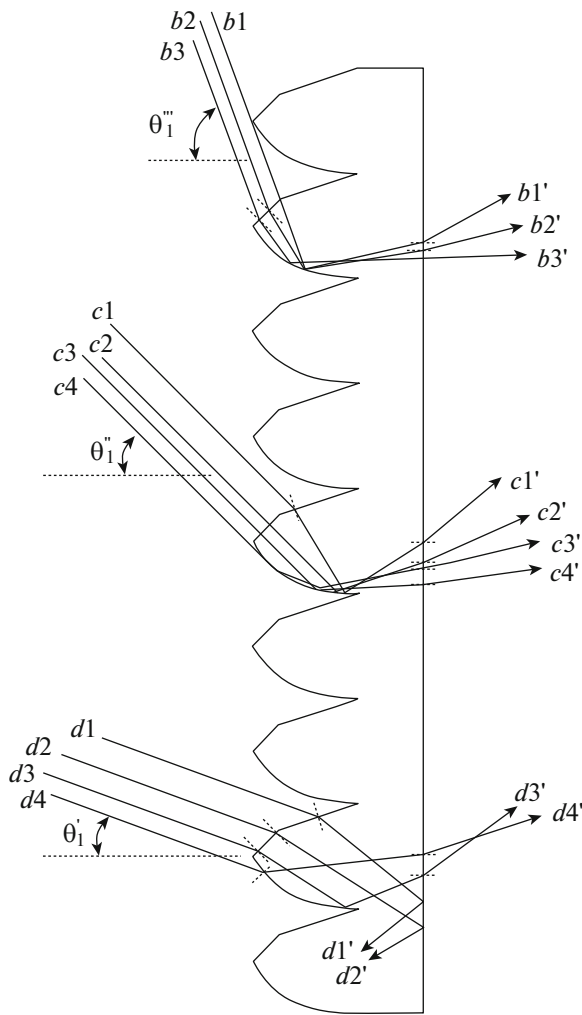


**Fig. 4.** Changes in the nature of the passage of parallel sun rays through a vertically located microprismatic structure of type 2 at a sequential increase in the angle of incidence  $\theta_1$  ( $\theta_1' < \theta_1'' < \theta_1'''$ ) [6].

It should be especially noted that the results here and below, except for those specified specifically, are given for the variant when the angle of the sun to the horizon  $\theta_1$  is located in the vertical plane normal to the vertical plane of the window. This state corresponds to the value of the azimuthal angle  $\varphi = 90^\circ$ . The specified planes coincide at  $\varphi = 0^\circ$ .

The incident sunlight consists of parallel rays. The type 1 microstructure redirects sunlight as a narrow weakly diverging ray of high intensity, forming a bright spot. As the sun rise angle increases, this flux shifts up to the ceiling and the bright spot moves throughout the day. Part of the sunlight is also directed downward as a narrow ray of high intensity. Downward-pointing light causes glare.

The type 2 structure diffuses light as a widely diverging flux of uniform intensity. The main part of the light is scattered upwards in the  $\theta_2$  angle range

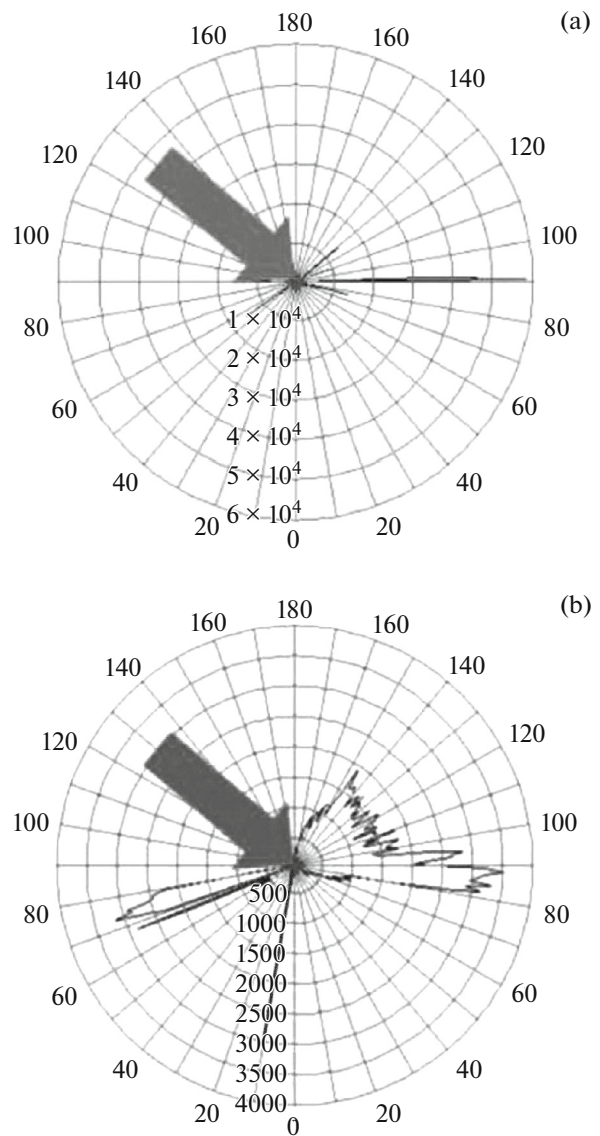


**Fig. 5.** Polar diagrams (indicatrices) of the scattering of incident sunlight at an angle of  $\theta_1 = 40^\circ$  to the horizon by vertically arranged microprismatic structures of (a) type 1 and (b) type 2 shown in Fig. 3 [6].

from  $90^\circ$  to  $160^\circ$ . A small part of the light in the range  $\theta_2 = 80^\circ - 90^\circ$  is redirected downward. The type 2 structure provides uniform natural illumination of a room of great depth when the sun moves during the day [6]. The distribution of light in the room is significantly affected by the ceiling, to which the redirected light is incident and from which it reflects. It should have a high reflectivity and scattering ability (white matte).

Figure 7 shows a cross-section of a microprismatic film, obtained using a scanning electron microscope. The microstructured film is produced using high-performance continuous roll-to-roll processing (R2R) at a speed of 3 m/min. First, a layer of prepolymer is

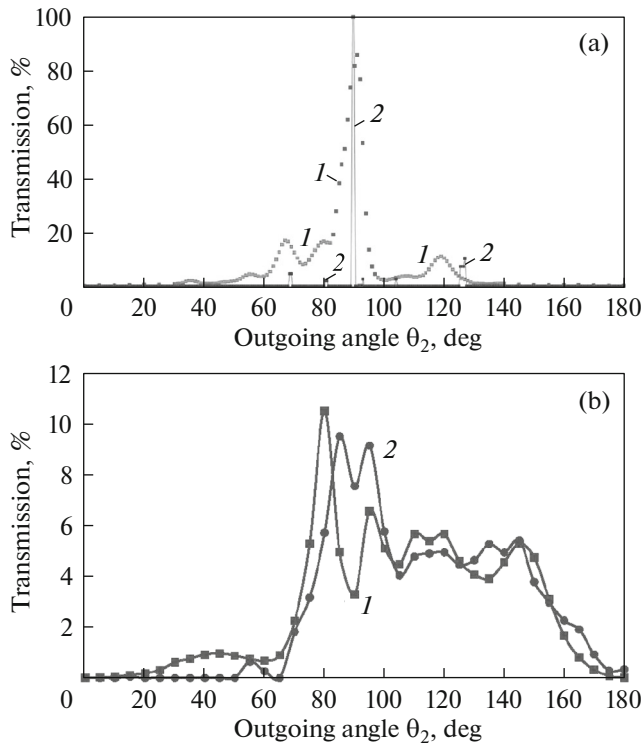


**Fig. 6.** (1) Experimental and (2) calculated results of the angular distribution of the intensity of sunlight passing through the microprismatic structures of (a) type 1 and (b) type 2 shown in Fig. 3, incident to them at an angle of  $\theta_1 = 40^\circ$  to the horizon [4]. The angle of radiation output  $\theta_2 = 0^\circ$  corresponds to the direction vertically down and  $\theta_2 = 180^\circ$ —vertically up.

applied to the polyethylene terephthalate (PET) film. Then, a microprismatic profile is squeezed out using a rotating matrix while photopolymerization is performed under the influence of high-density UV radiation of  $120 \text{ W/cm}^2$ . A roll of finished microprism film is shown in Fig. 8. An adhesion layer and protective removing film are applied to a flat surface.

A complex film with a microprismatic light-redirecting structure on one side and a nanostructured illuminating coating in the form of bumps  $127 \text{ nm}$  in height and  $330 \text{ nm}$  in diameter at the base and a spectral-selective silver coating  $15 \text{ nm}$  thick on the other side is also made using the roll-to-roll processing [6].

Somewhat later, with a delay of 2–3 years, the development of the 3M™ microprism film was performed by employees of the American company 3 M [7–9]. The results of studies of indoor lighting when using this film in the upper part of windows under field conditions are given in [10–12]. The description and characteristics of the 3M™ film microstructure is given in [12] and the detailed results of measuring its optical characteristics are reported in [11].

The 3M™ film microstructure is four-sided, similar in shape to the type 1 structure in Fig. 3. The

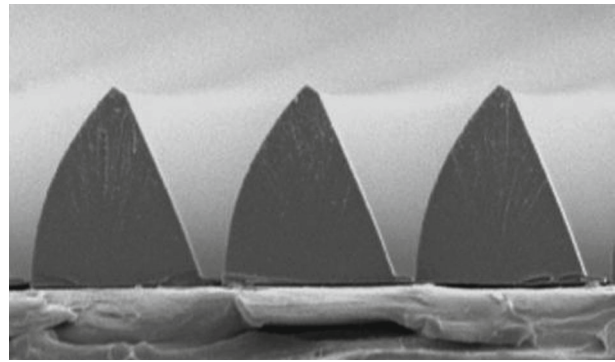


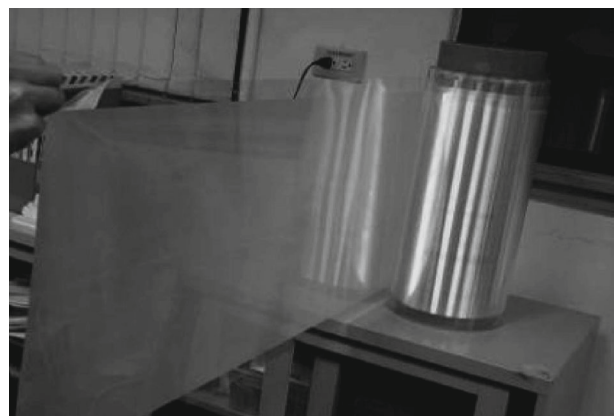
**Fig. 7.** A cross-section of a film with a prismatic microstructure of type 2 in a scanning electron microscope at a magnification of 1000 times [4].

microprism profile height  $H \sim 46 \mu\text{m}$  and pitch  $P \sim 30 \mu\text{m}$  [12].

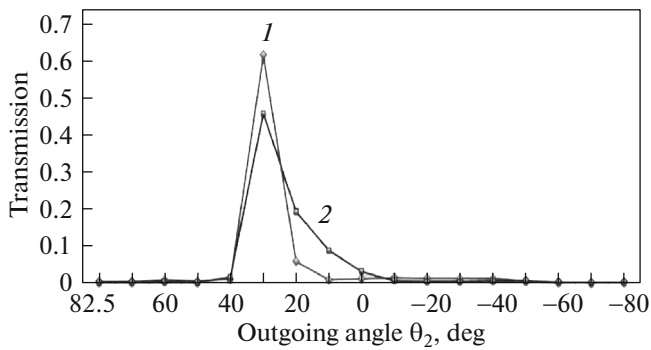
Because of the sufficient similarity in the geometric characteristics of the 3M™ and type 1 microprisms, the optical characteristics of the 3M™ microstructure film are also quite close to the similar characteristics of the type 1 structure.

Figure 9 shows the data on the light scattering by the 3M™ microstructure film when the sun is tilted to the horizon  $\theta_1 = 40^\circ$ . The similar data for the type 1 structure is shown in Fig. 6a. Various schemes of reading the angle of inclination of the redirected light was used. In Fig. 6a, the change in the direction from vertical down to vertical up corresponds to a change in the angle  $\theta_2$  from left to right from  $0$  to  $180^\circ$  while, in Fig. 9, the movement from bottom to top corresponds to a change in the angle  $\theta_2$  from right to left from  $-70^\circ$  to  $+82.5^\circ$ .

The 3M™ microstructure redirects sunlight as a sharp narrow high-intensity ray directed upwards at an angle of  $30^\circ$  to the horizon, forming a bright spot. For



**Fig. 8.** Roll of the finished film with a prismatic microstructure [4].



**Fig. 9.** (1) Experimental and (2) calculated results of the angular distribution of the intensity of sunlight passing through a 3M™ microprism film pasted on a vertical glass with a thickness of 3 mm, incident to it at an angle  $\theta_1 = 40^\circ$  to the horizon [11]. The angle of light output  $\theta_2 = 82.5^\circ$  corresponds to the direction up to the ceiling and  $\theta_2 = -70^\circ$ —down to the floor.

comparison, note that the type 1 structure redirects sunlight horizontally under these conditions.

When the sun rises at the angles  $\theta_2 > 20^\circ$ , the main part of the light coming out of the 3M™ microstructure is redirected upwards (curve 1 in Fig. 10). Figure 10 also shows the data (curve 2) describing the change in the light redirection when the vertical plane of the sun rays deviates from the vertical plane normal to the glass surface. When the azimuthal angle  $\varphi$  decreases from  $90^\circ$  to  $45^\circ$ , the tilt angle  $\theta_2$  to the horizon of the main part of the light coming out of the film decreases.

Because of the similarity in structural characteristics, the 3M™ film has the same disadvantage as the type 1 microstructure: the light comes out as a narrowly directed ray of high intensity. In addition, when using the 3M™ film, a faint iridescent halo appears because of the chromatic aberration inherent in prisms [10]. Therefore, it is recommended to additionally use a light scattering film to increase the uniformity of the redirected light distribution and eliminate the rainbow halo when using the 3M™ film [8–12]. In a double-glazed window, the 3M™ film is glued to the 2nd surface (the inner surface of the outer glass) and the light-scattering film is placed on the 3rd surface (the inner surface of the inner glass). When exposed to sunlight, a double-glazed window with two films looks from the inside as a luminous surface covered with frost.

The cost of the 3M™ film is about 233 €/m<sup>2</sup>.

### 1.3. Panels with Prismatic Microstructures on Two Surfaces

The LUMITOP® optical device that redirects sunlight is a set of concave transparent profiles made of PMMA, which are placed in a block between the glasses (Fig. 11). Profiles with a size of  $3.5 \times 12$  mm are

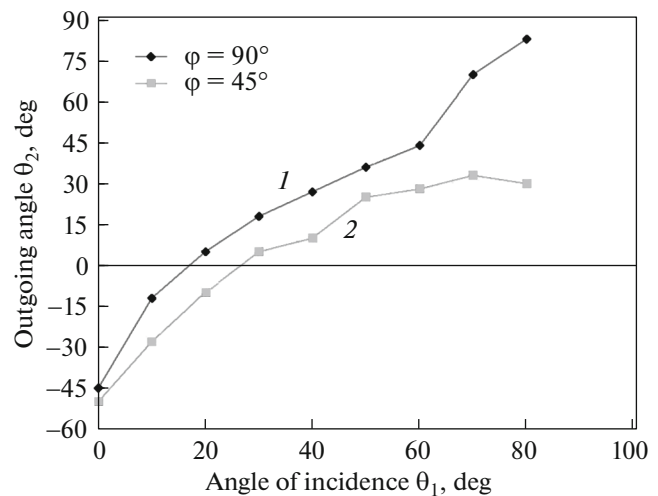


**Fig. 10.** Dependence of the angle  $\theta_2$  at which the main part of the light beam exit from the vertically positioned 3M™ microprismatic film on the angle  $\theta_1$  of the sun inclination to the horizon. The angle  $\theta_1$  of the sun inclination to the horizon is changed in (1) a vertical plane normal to the film surface  $\varphi = 90^\circ$  and in (2) a vertical plane at the azimuthal angle  $\varphi = 45^\circ$  to the film surface [11].

made by extrusion. Such products are produced by Saint-Gobain Glass [13].

The profiles of the elements are designed to redirect the incident sunlight in the range of angles from  $15^\circ$  to  $65^\circ$ , which corresponds to the conditions of Central Europe. The incident light is focused by the

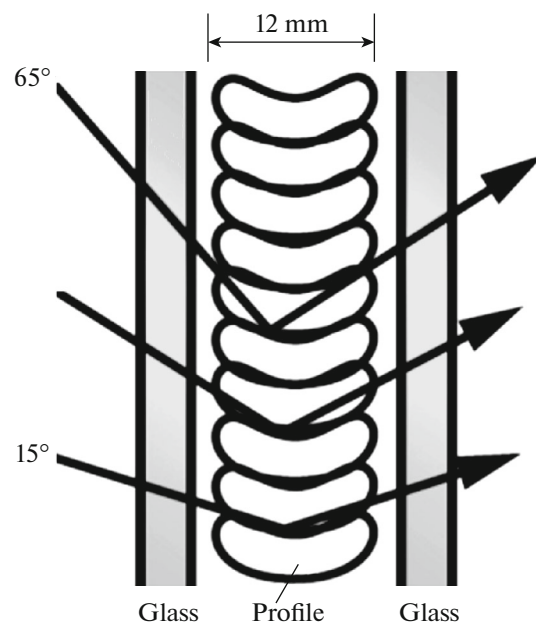


**Fig. 11.** Double-glazed window with a block of the LUMITOP® elements redirecting sunlight [13].

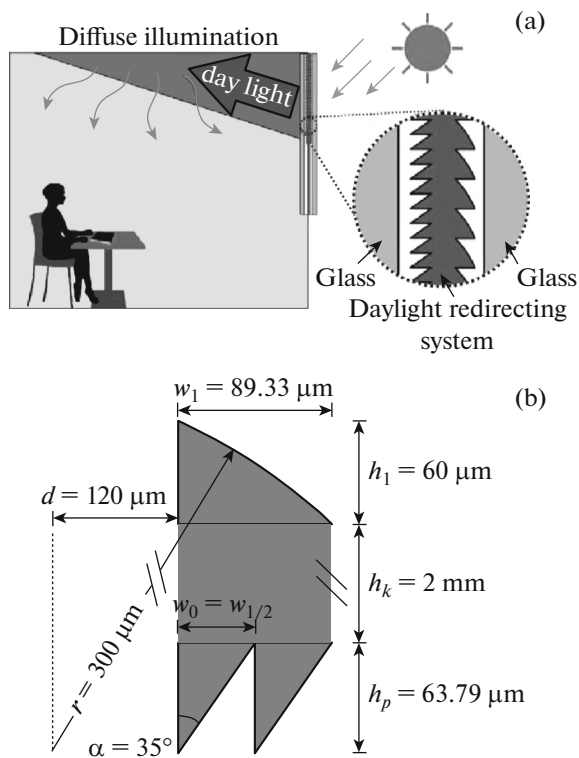


**Fig. 12.** (a) Layout and (b) cross-section of the panel with prismatic microstructures on the two sides [17].

first surface of the element, then, because of full internal reflection from the lower surface, it is directed up to the ceiling and from it to the depth of the room. The back edge of each profile is wavy for light scattering in the horizontal direction.

For effective natural lighting of rooms in a moderate climate, the double-glazed windows with the LUMITOP® element blocks should be placed in the upper part of the window and have a height of at least 10% of the room height. This device is not transparent to view from the inside. From the outside, it looks milky white.

Maximum dimensions of the LUMITOP® element blocks are 600 × 2600 mm. The blocks with a width of more than 600 mm are manufactured with a vertical dividing bar. The distance between the glasses is 24 mm. Additional (to the cost of a double-glazed window) cost of light-redirecting blocks of the LUMITOP® optical elements is about 200 €/m<sup>2</sup>.

The LUMITOP® device consists of composite elements and has a significant thickness and mass. A group of researchers in Germany set out to create a device for redirecting light with better optical characteristics in the form of a lighter solid panel of a smaller thickness. In addition, the solid panel serves as an additional glass in the double-glazed window, which improves its thermal properties. Long-term exploratory development of a panel with optical microstructures

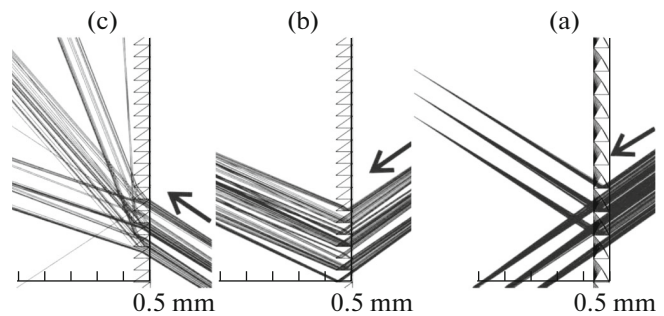


**Fig. 13.** Distribution of the sunlight beams falling from the right at the angle  $\theta_1 = 35^\circ$  to the horizon when passing through a panel with prismatic microstructures on two sides [17]. The arrows show the direction of the light.

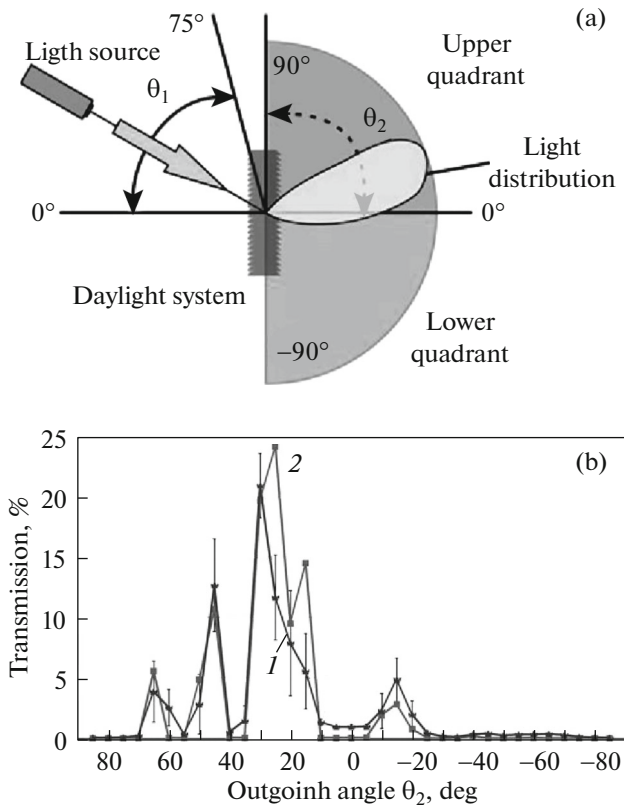
tures on both sides [14–17] was completed and put into practice during the four-year 2016–2019 state program “TaLED” (Energy- and cost efficient, facade integrated Day- and LED lighting based on micro-optical components) at the cooperation of scientific, industrial, and architectural organizations [18].

Figure 12 shows the layout and cross-section of the developed panel with prismatic microstructures on both sides. There is a lenticular microstructure on the outer (solar) side of the panel and a three-sided one—on the inner side. The panel thickness is 2 mm. The lenticular structure has a pitch of 89.33 μm, a height of 60 μm, and a rounding radius of the cylindrical surface of 300 μm. The three-sided microprisms with a height of 63.79 μm have a half-step of 44.67 μm on the inner side of the panel.

Figure 13 shows the results of calculating the course of incident light rays from the right at an angle  $\theta_1 = 35^\circ$  to the horizon. A lens-like microstructure on the outer surface divides the incident light into two focused rays: one passes downward and the second, after a complete internal reflection from a horizontal flat face, is directed upward. The microstructure on the inner surface dissipates and redirects the bulk of both flows upwards. The panel thickness should be at least two focal lengths of the lens-like structure. This allows you to avoid the undesirable effect of a sharp change in the direction of the outgoing light at a small change in the inclination of the incident light, inherent in prismatic structures with flat faces.

The optical characteristics of a panel with prismatic microstructures on two sides are shown in Fig. 14. The diagram for performing measurements and counting angles is shown in Fig. 14a. The angle of light output from the device  $\theta_2 = 90^\circ$  corresponds to the direction vertically up and the angle  $\theta_2 = -90^\circ$  corresponds to the direction vertically down.

The device divides the sunlight incident at an angle of 45° into four diverging beams (Fig. 14b). Three of



**Fig. 14.** Optical properties of a panel with prismatic microstructures on two sides [16]. (a) Measurement scheme using a goniophotometer. (b) (1) Experimental and (2) calculated results on the angular distribution of the sunlight intensity at the exit from the panel when it falls at the angle  $\theta_1 = 45^\circ$  to the horizon.

them, containing the main part of the light, are directed up and the fourth, which is of low intensity, is directed down.

The main part of the light is directed upwards when the angle  $\theta_1$  of the sun rise changes from  $10^\circ$  to  $65^\circ$  (Fig. 15). And over the entire range, a panel with two micropismatic surfaces redirects upwards on average about 25% more light than a LUMITOP® device.

If there are indicatrices of the light scattering by different prismatic microstructures, it is possible to compare the nature of scattering the sunlight incident at a same angle of  $40^\circ$  by them. Such data are given for a micropismatic four-sided structure with a single curved face (type 2) in Fig. 6b, for a four-sided micropismatic structure with flat faces (type 1) in Fig. 6a, for a four-sided micropismatic structure with flat faces (3M™) Fig. 9, and for a panel with prismatic microstructures on two sides in Fig. 14b. The microstructures with a single curved face have the best properties: they produce an upward flux of uniform intensity with a large opening angle (Figs. 6b and 14b).

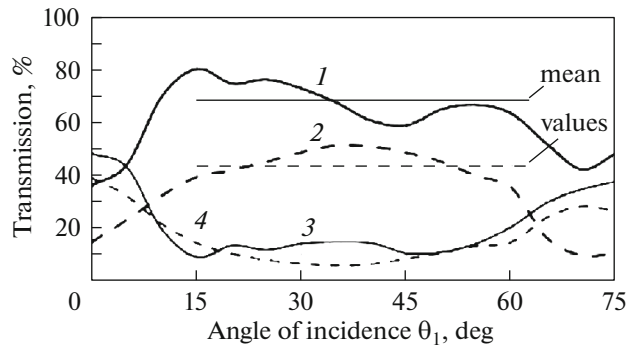


**Fig. 15.** The sunlight proportions directed (1, 2) up and (3, 4) down after (1, 3) a panel made of polydimethylsiloxane (PDMS) with prismatic microstructures on two sides and (2, 4) the LUMITOP® element block [16].

## 2. PANELS AND FILMS WITH MICROMIRRORS

### 2.1. Laser-Cut Panels

Laser-cut panels are made by cutting slits-incisions in a transparent PMMA plate with a thickness of about 5 mm by a laser beam (Fig. 16). Under the influence of a laser beam, the polymer melts and evaporates to form polished surfaces. Each surface becomes a small mirror that reflects the light passing through the panel

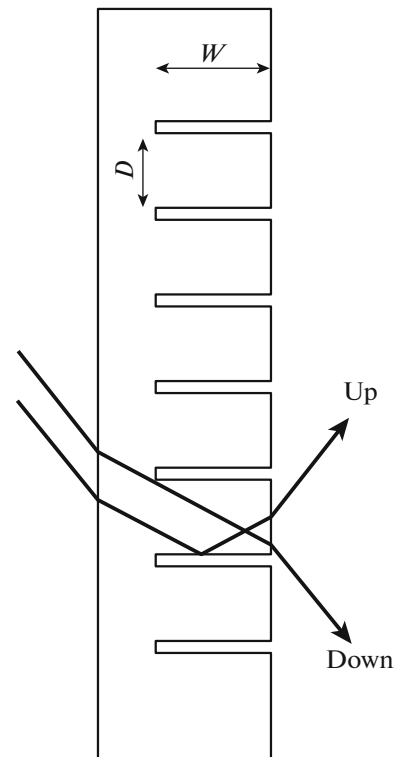


**Fig. 16.** Splitting of sunlight in a laser-cut panel [19].

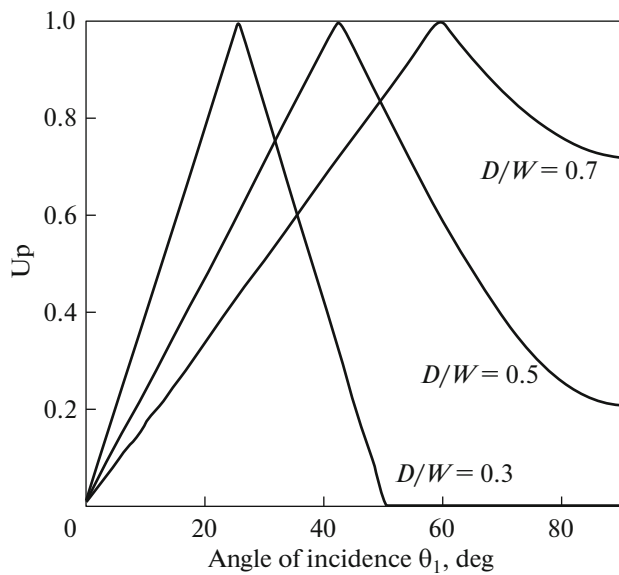


**Fig. 17.** Dependence of the up-redirection part of light on the angle of sun rise for the panels with different  $D/W$  ratio [19].

because of full internal reflection. The grooves can be made in two ways [19]:

- cut to the specified depth;
- through cutting of the plate followed by its lamination with another thin plate made of the same material.

In both versions, you should leave solid lintels of 20–30 mm to ensure the structural integrity of the panel. Then the laser-cut panel is laminated between two thin 1.0–1.5 mm thick glasses. The advantage of this panel is its high transparency: when viewed through it at a normal angle to the surface, the image is almost not distorted.

The light flux entering the plate is divided into two parts: one part (Down) passes down without changing the direction and the second one (Up) experiences a complete internal reflection from the surface of the slits and goes up at the same angle to the horizon.

The ratio between the fractions of light passing through the plate is determined by two parameters:

- the tilt angle  $\theta_1$  of sunlight to the horizon;
- the ratio  $D/W$  between the depth  $W$  of the grooves and the distance  $D$  between them.

Figure 17 shows the change in the proportion of the upward-directed light flux depending on its angle of incidence for three geometric characteristics. In all variants, the proportion of the light stream redirected upwards initially increases to the limit value with the angle of incidence. In this case, all light passing through the plate is redirected upwards. The value of the corresponding angle  $\theta_1$  depends on the geometric parameters: the smaller the distance between the

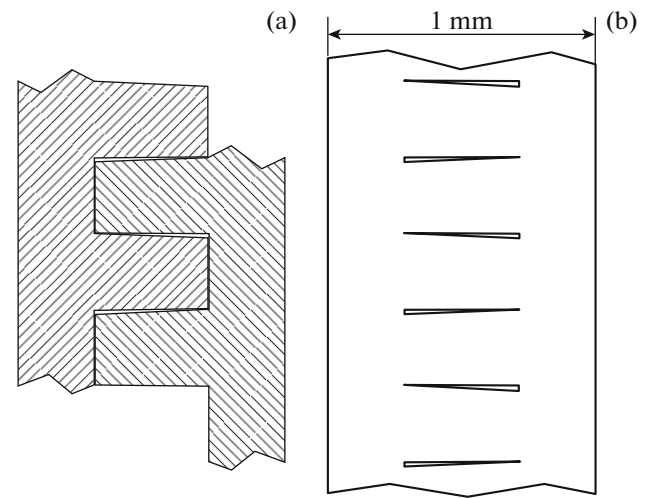


**Fig. 18.** (a) Workpieces and (b) finished product of SerraGlaze® [23].

grooves at the same depth, the smaller the value of the angle  $\theta_1$  at which it occurs. By changing the geometric parameter  $D/W$  for the specified conditions (angle  $\theta_1$ ), you can choose the best option for redirecting light to the ceiling.

It should be especially emphasized that the most important geometric characteristic of such a product is not the absolute dimensions  $D$  and  $W$ , but the ratio between them  $D/W$ .

Laser-cut acrylic panels with a thickness of 2 to 20 mm laminated with glass cost about \$100/m<sup>2</sup> are produced by the Australian company SOLARTRAN [20].

## 2.2. SerraGlaze® Plates with Micro-Slits

Laser-cut panels in a reduced size are embodied in the form of a micro-slit SerraGlaze® plate manufactured by SerraLux Inc [21]. “Serra” stands for Stacked Elemental Refractor/Reflector Array. The product design is protected by the main patent [22]. A detailed description of the manufacturing technology and the main characteristics of the plate are given in [23].

The structure of the plate is shown in Fig. 18. Grooves-protrusions of a shape close to a rectangular one are accurately extruded in the initial heated PMMA plate with a thickness of 0.5 mm and dimensions of 300 × 300 mm using the microreplication technique. The height of the protrusions is ~0.5 mm and the thickness—~0.3 mm. The tops of the protrusions are smeared with an ultra-thin (several microns) layer of photopolymerized adhesive composition and two plates made in this way are inserted into each other. In this case, the tops of the protrusions fit tightly and triangular micro-slits with an average thickness of ~10 μm are formed between the side sur-



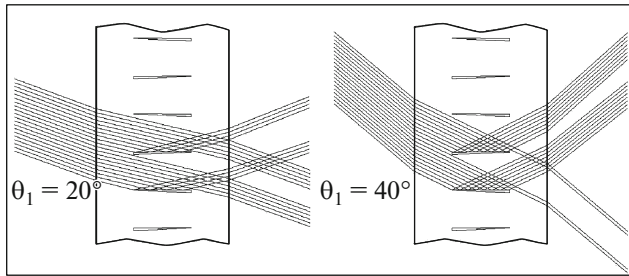


**Fig. 19.** Splitting of sun rays incident at different angles to the SerraGlaze® plate [23].

faces of the protrusions. As a result, a solid monolithic plate with a thickness of  $\sim 1$  mm with numerous internal micro-slits is obtained after lamination and photopolymerization of the glue. Manufactured square plates are laid out in a mosaic, both sides are covered first with a sticky film and then with glasses, and laminated. The finished product SerraGlaze® is a multi-layer composite glass with a PMMA plate mounted in the center with numerous horizontal micro-slits.

When a light beam falls on the surface of a horizontal micro-slit, it is reflected from it as a result of complete internal reflection. Figure 19 shows the course and splitting of light rays inside such a plate. Part of the light flux does not change its direction and another part is reflected symmetrically upwards. The proportion of light redirected upwards increases with the angle of incidence.

A more complete understanding of the quantitative relationship between the light fluxes passing through the plate can be obtained from the data shown in Fig. 20. The light incident horizontally passes almost completely (85%) through the plate. This indicates that when viewed horizontally through the plate, the image is practically not distorted. The proportion of light redirected upwards increases with the angle  $\theta_1$  because of a reduction in the proportion of the light passing without changing the direction. The slope of the straight line that determines the ratio between the shares of redirected and non-directional light depends on the ratio between the length of the slits and the distance between them ( $D/W \sim 0.6$  for the data in Fig. 20).

The disadvantage of laser-cut panels and SerraGlaze® plates with micro-slits is that they redirect light upwards in a parallel stream creating a bright spot on the ceiling (glare). In addition, the range of the angles  $\theta_1$  of the sun inclination in which light is redirected upwards (a narrow sharp triangular peak) is narrow and the proportion of this light is small (Figs. 17 and 20). These disadvantages are clearly evident when comparing the results for these panels (Figs. 17 and 20) and the results for LUMITOP® devices and panels with prismatic microstructures on two sides in Fig. 14.

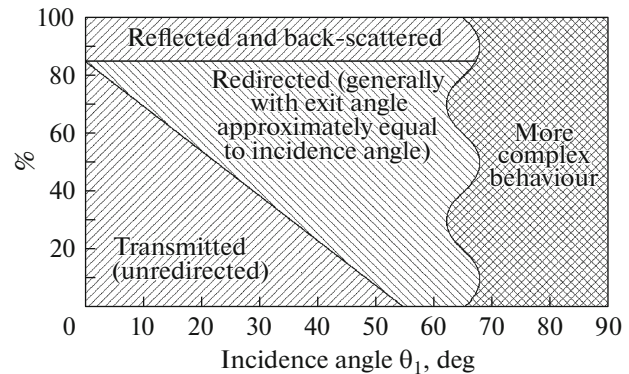


**Fig. 20.** Changing the ratio between the fractions of directed, redirected, and reflected sunlight when passing through the SerraGlaze® plate, depending on the angle of incidence [23].

### 2.3. Films with Embedded Micro-Mirrors

Laser-cut panels obtained further development in the direction of miniaturization in the form of a polymer film with embedded micro-mirrors, proposed by a group of Swiss researchers [24]. Reducing the thickness to less than 1 mm and the film flexibility allow you to stick it on the glass, thereby greatly simplifying the design and manufacture of double-glazed windows.

The polymer film with embedded micro-mirrors is shown in Fig. 21a. The parabolic micromirrors 2, the focus of which is on the flat micromirrors 3 located on the outer surface of the film, are embedded in a polymer film 1. Approximate product dimensions: film thickness is  $\sim 0.5$  mm; the length of the parabolic micromirror is 100–300  $\mu\text{m}$ ; the distance between micromirrors is equal to about half their length; and the height of the vertical micromirrors is 20–40  $\mu\text{m}$ .

The flat mirrors in laser-cut panels and SerraGlaze® products direct the reflected solar radiation upwards in a parallel flax, which creates a bright spot with a large light gradient and glare. To eliminate this defect, parabolic micromirrors were proposed (Fig. 21a). In winter, a parallel sunlight flux directed at an angle of  $25^\circ$  to the horizon fell on a parabolic mirror surface, reflected at various angles, and scattered. As a result, a diverging beam of scattered light, which evenly illuminates the ceiling and the far wall of the room, comes out of the film.

In summer, when the sun is high, the light reflected by the parabolic micromirror 2 focuses on the surface of the vertical micromirror 3 and is reflected back. This eliminates overheating of the room. The combination of two micromirrors provides uniform redirection of scattered sunlight and almost zero transmission at selected angles of sun rise around  $60^\circ$ , thus providing natural lighting and seasonal control of heat input.

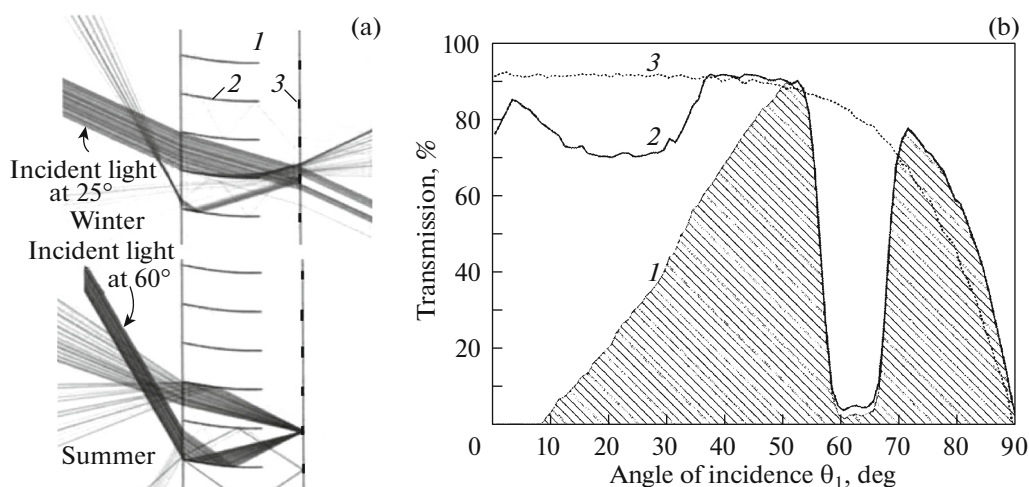


**Fig. 21.** Optical properties of the film with embedded micromirrors [24]. (a) Structure of the polymer film and calculated results of the direction of sunlight rays in winter and summer: (1) polymer film, (2) parabolic micromirror, and (3) flat micromirror. (b) The transmittance of the film at different angles  $\theta_1$  of the sun above the horizon: the (1) part of upward scattered light, (2) full light transmission of the film, and (3) light transmission of colorless glass with a thickness of 3 mm.

The optical characteristics of the film with embedded micromirrors are shown in Fig. 21b. A slight decrease in light transmission at the sun elevation angles in the range  $0 < \theta_1 < 30^\circ$  is caused by the reflection from vertical micromirrors. At the same time, the small transverse dimensions of micromirrors make them invisible to the naked eye. Therefore, these films when viewed through them look transparent and evenly shaded compared to colorless glass. The proportion of up-directed scattered light increases linearly with the sun rise starting from about  $\theta_1 = 10^\circ$  because of a decrease in the proportion of down-directed parallel flux. At  $\theta_1 > 50^\circ$ , all light is scattered upwards. The failure of light transmission in the range of  $55^\circ < \theta_1 < 70^\circ$  is caused by the reflection from vertical micromirrors. In the absence of these micromirrors, there is also no light transmission failure.

It should be noted that the optical characteristics of a film with embedded micromirrors in Fig. 21b are similar to those of laser-cut panels (Fig. 17) and Serraglaze® products (Fig. 20). But there is a qualitative difference: in the first case, scattered light is directed upwards, while, in the other two, a directed light beam is reflected upwards.

The calculations performed showed that natural lighting in sunny weather significantly improves in rooms where single-chamber double-glazed windows with films with embedded micromirrors glued on the upper (one- or two-thirds) part of the glass are installed [25]. In these rooms, the uniformity of lighting along the room improves, the illumination in the depth increases, and the probability of glare decreases in comparison with the rooms with the same double-glazed windows without films.

The films with embedded micromirrors have good optical properties. The problem is in their manufacture. To do this, a series of operations should be performed sequentially: forming a polymer microprismatic film one of the faces of which has a parabolic profile, spraying a metal mirror coating on a face with a parabolic profile, filling the microprismatic structure with the same polymer material to form a smooth surface on its other side, and spraying an external metal mirror coating [24]. Until recently, technological difficulties have not been overcome. The main problems arise in the manufacture of a metal matrix for forming a film with microstructural parabolic profiles. Only small film samples (no more than  $25 \times 45$  mm) and without external mirrors were obtained in the course of fairly long development [24, 26, 27]. One of the reasons is the use of the technology that is applicable to the manufacture of flat products. Previously, it was noted that the roll-to-roll (R2R) technology allows us to produce a film of a complex structure with a microprismatic light-redirecting structure on one side and a nanostructured illuminating coating in the form of bumps with 127 nm in height and 330 nm in base diameter and a spectral-selective silver 15 nm thick coating on the other side [6].

### 3. SWITCHABLE MICRO-MIRRORS AND MICRO-BLINDS

Optical microelectromechanical systems (MEMS) are microdevices containing a movable part whose position is controlled by electrostatic forces between two electrodes in these elements. Optical MEMS are manufactured using microelectronics technologies. Micromirrors, are electrically switched miniature mir-

**Table 1.** Structural and optical properties of arrays of micro-blinds and micromirrors

Electrical insulator	A movable electrode	Micro-flap dimensions, $\mu\text{m}$	Active area, $\text{cm}^2$	$\tau^+/\tau^-$ , %	Activation voltage, V	Literature
—	—	$458 \times 2500$	—	—	80	[30]
$\text{SiO}_2$	$\text{SiN}_x/\text{SiO}_2/\text{Al}/\text{SiO}_2/\text{SiN}_x$	$150 \times 400$	100	75/2	40–80	[35]
$\text{SiO}_2$ , $\text{SiN}_x$ , $\text{Al}_2\text{O}_3$	Cr and others, 100 nm	$50 \times 150$ ; $100 \times 150$	20	60/0.1	15–25	[34]
$\text{SiO}_2$ , 200 nm	$\text{SiO}_2$ , 200 nm/Al, 100 nm	$200 \times 30$	0.25	53/36	55	[33]

$\tau^+/\tau^-$  is the ratio of light transmission in the open  $\tau^+$  and closed  $\tau^-$  states.

rors with dimensions in the range of 10–1000  $\mu\text{m}$ , are the mostly widely used.

The first digital micromirror devices were developed in the late 1980s for modulating light in video projectors and optoelectronics devices [28]. Such devices are made in the form of an array of micromirrors that are electrostatically deflected between two positions: “on” and “off,” at an angle of  $10^\circ$ – $12^\circ$ . These devices have been used in multimedia projectors, optical switches, and astronomical telescopes.

Digital micromirrors manufactured by Texas Instruments contain more than 2 million ( $2048 \times 1080$ ) micromirrors with the dimensions of the order of  $10 \times 10 \mu\text{m}$ . Micromirror arrays containing 2048 ( $32 \times 64$ ) electrostatically controlled micromirrors were made for a multi-purpose spectroscope [29]. Each micro mirror has a size of  $200 \times 100 \times 10 \mu\text{m}$  and is deflected by an angle of  $25^\circ$  under the action of a voltage of 130 V.

Later, in the early 2000s, optical MEMS was proposed to be used to control the light flux through glasses: in electrically switched (dynamic) glasses. This was done by groups of researchers in several countries [30–33]. Some researchers limited themselves to a single publication of the results. The groups in Canada [32, 34] at the University of Kassel in Germany [31, 35–38] continue their researches. Detailed results are published in the form of a report [35], articles [36, 37], and a dissertation [38].

Two variants of optical MEMS are proposed: micro-blinds [30, 32, 33] and micromirrors [31]. Figure 22 shows images of these devices. In the “open” state, the micro-blinds are rolled up and the flat micromirrors are bent at an angle close to a straight one. When connecting the voltage to the electrodes, both devices under electrostatic influence are straightened, adjacent to the glass, and close the micro holes “closed.” The miniaturization of optical elements allows them to be invisible to the naked eye and significantly increase their service life.

The technology of manufacturing micro-blinds includes five operations for applying thin-layer coatings and two operations for structuring them using photolithography (Fig. 23). The upper electrode of the micro-blind is usually made two-layer to create internal stresses, under the influence of which the micro-

blind is rolled up after removing the sacrificial layer. When connecting the voltage between the electrodes, the micro-blinds are unrolled under electrostatic influence and close the micro-hole and the micromirrors are unbent and adjacent to the glass.

The main characteristics of optical MEMS are shown in the Table 1.

It is much more difficult to make a micromirror than a micro-blind: it is necessary to provide a flat deflected surface rather than a rolled up one. But they also have a number of significant advantages because of the flat shape of the micromirror.

The structure of the first micromirrors and their interaction with the sunlight flux in the closed and open states is shown in Figs. 24, 25. Here, the mirror is made of five layers. The light is reflected from the aluminum mirror layer. The improvement of manufacturing technology and the structure of flat deflected micromirrors has been continued for more than 15 years [31, 35–38].

To make the micromirror shown in Figs. 24, 25, you have to perform eight thin-layer coatings operations and three operations of their structuring using photolithography. Micromirror consists of several layers of different materials. A multi-layer structure is required:

- to create a pre-stressed state on the hinge section of the micromirror: the hinge section is bent under internal stresses after removing the sacrificial layer;

- to ensure the flat shape of the main part of the mirror.

Each micromirror is anchored to the glass. The anchor part is an electrical conductor that connects the aluminum mirror layer to the power source.

In the free state, the micromirror is bent away from the glass. The hinged part makes the micromirror movable. When an electric field is created between an electrically conductive translucent layer and a metal mirror layer as a result of voltage connection, electrostatic forces of attraction arise between the layers, under the action of which the micromirror is attracted to the glass surface. When the electric field is switched off, the hinge part bends under the action of uncompensated internal stresses and the micromirror moves away from the glass.

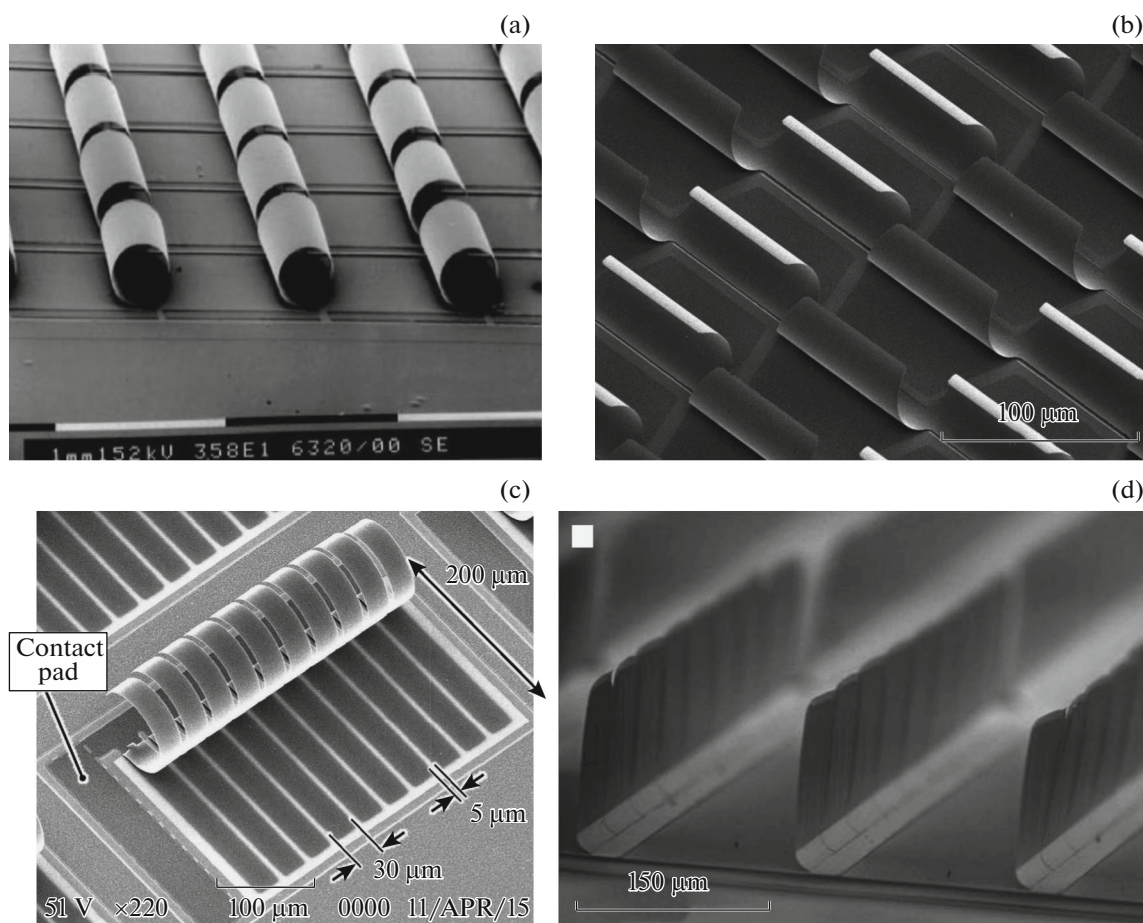


**Fig. 22.** Images of the optical microelectromechanical systems in an open state in scanning electron microscope: (a) micro-blinds [30], (b) micro-blinds [34], (c) micro-blinds [33], and (d) micromirrors [38].

Theoretical calculations have shown that under the action of electrostatic forces, as the voltage increases from 0 to 80 V, the micromirror from the initial position with an angle of inclination to the plane of the glass  $\sim 90^\circ$  controllably tilts towards the glass up to an angle of  $\sim 45^\circ$  [35, 36]. At a further increase in voltage, the micromirror tilts uncontrollably to the glass, closes it, and is fixed in this position. However, it has not been possible to provide experimentally intermediate states of micromirrors with an adjustable slope from  $90^\circ$  to  $45^\circ$  to date: only the extreme states “open” and “closed” are implemented. Figure 22d shows an image of an array of micromirrors in the open position.

Prototypes of  $100 \times 100$  mm micromirror arrays were made. The size of a single micromirror was  $150 \times 400$   $\mu\text{m}$ . About 12 micromirrors are placed on a  $1 \text{ mm}^2$  site and about 120000 such elements are placed on a  $100 \times 100$  mm sample. The glass area of  $1 \text{ m}^2$  will fit 12000000 pieces. In order to keep the array of micromirrors in a closed state, it is necessary to spend electrical power of  $1 \text{ mW}/\text{m}^2$ . Light transmission is 75% in the open and 2% in the closed states.

Since the eye cannot distinguish individual micro-lights, the image is not distorted when viewed through a sample with open micromirrors, but the array of micromirrors is evenly shaded like in the case of the addition of a thin-film shading coating. In the micromirror open state, part of the light passes without changing the direction and the other part is redirected to the ceiling and increases the uniformity of lighting in the room. The sample with closed micromirrors practically does not pass light.

The only way to regulate light transmission is to produce an array of micromirrors in the form of selectively activated rows-submassives.

Micromirrors are rolled up in the normal position without electrostatic influence: the state “open.” When the voltage is connected, they unroll under electrostatic influence and go into a flat state: a “closed” one. Micro-blinds do not redirect incident light to the ceiling. It is only possible to change the light transmission by closing part of them, which is achieved by making a sequence of rows of micro-blinds of different sizes. Micro-blinds in such rows are closed under the action of various voltages: the larger the size of the

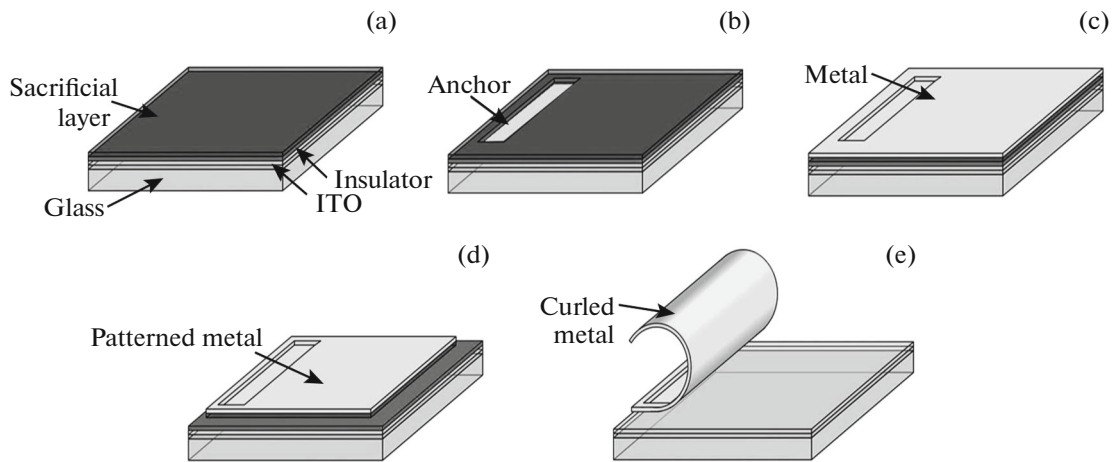


**Fig. 23.** A typical scheme for manufacturing micro-blinds [34]. (a) A glass substrate with successive layers of the lower electrode made of transparent conductive oxide ITO (ITO stands for Indium Tin Oxide  $\text{In}_2\text{O}_3:\text{Sn}$ ), the insulator ( $\text{SiO}_2$ ), and sacrificial layer; (b) structuring the sacrificial layer by photolithography to free the anchor attachment points; (c) sputtering the upper two-layer electrode; (d) structuring the upper electrode by photolithography; and (e) releasing the micro-blinds by removing the sacrificial layer.

micro-blinds, the greater the value of the voltage required for closing them [32, 39].

Micromirrors are activated electrostatically and are so small that the naked eye cannot distinguish them individually from a distance of more than 0.20 m, resulting in the impression of a uniform panel. The main advantages of the micromirror array:

- high switching speed;
- low power consumption, which is significantly less than for other types of dynamic glasses;
- light is not absorbed, but is completely reflected to the ceiling of the room or outside, so there is no heating of the glass, unlike in the case of thermochromic and electrochromic devices based on radiation absorption;

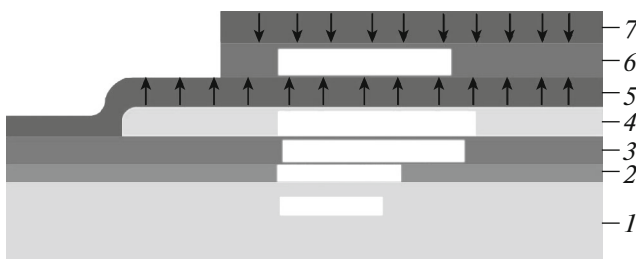


**Fig. 24.** A variant of the micromirror structure [35]: (1) glass, (2) transparent conductive layer, (3) electrically insulating layer ( $\text{SiO}_2$ ), (4) sacrificial layer, (5) dual-layer support layer (micromirror base) that consists of layers of silicon nitride  $\text{SiN}_x$  and silicon dioxide  $\text{SiO}_2$ , (6) aluminum mirror layer, and (7) compensating layer (similar to the inverted support one) that consists of layers of dioxide and silicon nitride. The arrow is a conventional image of the internal stresses.

—they do not change the spectrum of sunlight, but reflect near-infrared radiation by an ITO layer;

—despite the use of mechanically movable elements, the service life is long because of their miniaturization.

Micromirrors cannot completely replace competitive technologies of switchable glasses or light modulators. However, they are the best candidate for the applications where switching-light modulation speed, low power consumption, contrast, operating time, and temperature stability are essential.

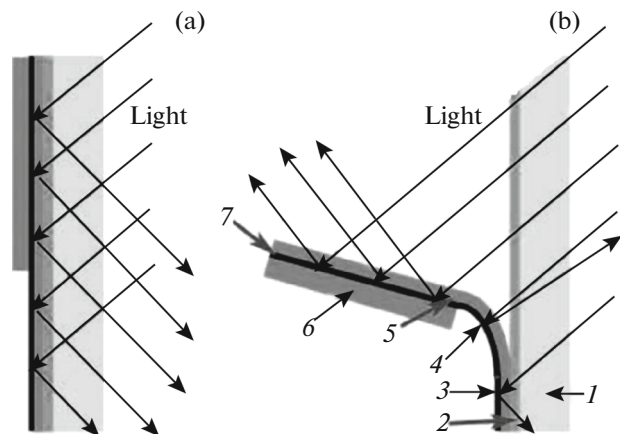


**Fig. 25.** The scheme of interaction of sunlight with micro-mirror in the (a) closed and (b) open states [35]: (1) glass, (2) insulating layer deposited on the transparent conductive layer, (3) the anchor part that is a part of the circuit, (4) the hinge part, (5) the support layer (micromirror base), (6) compensating layer, and (7) an aluminum mirror layer.

The main drawback of the micromirror array is the limitations on its size, which are imposed by the rather complex technology of microelectronic systems used for manufacturing. The maximum implemented size of the micromirror module is  $100 \times 100$  mm [37]. Such modules are combined into arrays to increase the size of dynamic glasses. Improving the technology will lead to a gradual increase in the size of micromirror modules and reduce their cost to the values at which they can be installed to regulate the light flux in windows.

#### 4. CONCLUSIONS

A significant reduction in electricity and an increase in the uniformity of illumination is achieved when using optical devices placed in lateral natural lighting systems in the upper part of the window in order to redirect sunlight to the reflecting ceiling and into the interior of the room.

The initially proposed optical devices have a number of disadvantages because of their significant weight and dimensions. Currently, research is being conducted to improve window optical devices by reducing their size to the micro level. Reducing the size of optical structures does not change their optical properties and avoids deviations from the laws of geometric optics as long as their dimensions do not reach the visible light wavelength range. Moving optical structures to the micro level makes it easier to embed them in windows and reduces the visual impact they cause.

Three types of window optical microstructures were developed and studied: microprismatic films, panels with prismatic microstructures on two sides, and films with embedded micromirrors. The development of microprismatic film has reached the stage of commercial implementation: it is manufactured using high-performance continuous roll-to-roll (R2R) technology, is easily mounted by gluing on glass, and has passed full-scale tests. The microprismatic film with curved surfaces instead of flat ones provides a high uniformity of the redirected scattered sunlight flux.

Arrays of micromirrors and micro-blinds, which are optical microelectromechanical systems manufactured using microelectronics technology, have specific properties. However, technological problems limit the geometric dimensions of these devices.

Significant efforts are needed to bring various types of window optical microstructures to the stage of commercial implementation. It is hoped that this review provides a complete picture of the current state of research in this area and arouses interest in further expanding it.

#### CONFLICT OF INTEREST

The author states that there is no conflict of interest.

#### REFERENCES

1. N. Ruck, Ø. Aschehoug, S. Aydinli, J. Christoffersen, G. Courret, I. Edmonds, R. Jakobiak, M. Kischkoweit-Lopin, M. Klinger, M. Lee, L. Michel, J. L. Scartezzi, and S. Selkowitz, *Daylight in Buildings: A Source Book on Daylighting Systems and Components, A Report of IEA SHC Task 21/ECBCS Annex 29, July 2000* (Int. Energy Agency, CA, 2000).
2. W. Lorenz, *Solar Energy* **70**, 109 (2001).  
[https://doi.org/10.1016/S0038-092X\(00\)00132-8](https://doi.org/10.1016/S0038-092X(00)00132-8)
3. Siteco Daylight Systems.  
<http://www.siteco.com/en/products/daylight-systems.html>.
4. H. Hocheng, T. Y. Huang, T. H. Chou, and W. H. Yang, J. Achievem. Mater. Manuf. Eng. **43**, 409 (2010).
5. H. Hocheng, T. Y. Huang, T. H. Chou, and W. H. Yang, *Energy Build.* **43**, 1011 (2011).  
<https://doi.org/10.1016/j.enbuild.2010.12.027>
6. T. Y. Huang, H. Hocheng, T. H. Chou, W. H. Yang, C. J. Ting, K. Y. Cheng, and C. W. Hsieh, *Energy Build.* **90**, 114 (2015).  
<https://doi.org/10.1016/j.enbuild.2014.12.051>
7. R. Padiyath, *Daylight Redirecting Window Films, EST-CP Project EW-201014, Final Report* (3M Company, 2013).  
<https://www.serdp-estcp.org/Program-Areas/Energy-and-Water/Energy/Conservation-and-Efficiency/EW-201014>.
8. R. Padiyath, B. Hao, and C. A. Marttlla, US Patent No. 8995059 B2 (2015).
9. 3M™ Daylight Redirecting Film.  
<https://multimedia.3m.com/mws/media/1209715O/3m-daylight-redirecting-film.pdf>.
10. A. Thanachareonkit, E. S. Lee, and A. McNeil, *LEUKOS: J. Illum. Eng. Soc. North Am.* **10**, 19 (2014).  
<https://doi.org/10.1080/15502724.2014.837345>
11. A. McNeil, E. S. Lee, and J. C. Jonsson, *Build. Environ.* **113**, 280 (2017).  
<https://doi.org/10.1016/j.buildenv.2016.07.019>
12. Z. Tian, Y. Lei, and J. C. Jonsson, *Build. Simul.* **12**, 129 (2019).  
<https://doi.org/10.1007/s12273-018-0487-z>
13. SGG LUMITOP. Saint-Gobain Glass. [www.saint-gobain-glass.com](http://www.saint-gobain-glass.com).
14. G. Walze, P. Nitz, J. Ell, A. Georg, A. Gombert, and W. Hossfeld, *Sol. Energy Mater. Sol. Cells* **89**, 233 (2005).  
<https://doi.org/10.1016/j.solmat.2004.11.016>
15. S. Klammt, H. Müller, and A. Neyer, in *Convention Proceedings of PLDC 2nd Global Lighting Design Convention, Berlin, 2009*.
16. S. Klammt, A. Neyer, and H. F. O. Mueller, *Solar Energy* **86**, 1660 (2012).  
<https://doi.org/10.1016/j.solener.2012.02.034>
17. M. Jakubowsky and A. Neyer, *Energy Proc.* **122**, 157 (2017).  
<https://doi.org/10.1016/j.egypro.2017.07.338>
18. H. F. O. Mueller, *J. Daylighting* **6**, 52 (2019).  
<https://doi.org/10.15627/jd.2019.7>
19. I. R. Edmonds, *Sol. Energy Mater. Sol. Cells* **29**, 1 (1993).  
[https://doi.org/10.1016/0927-0248\(93\)90088-K](https://doi.org/10.1016/0927-0248(93)90088-K)

20. SOLARTRAN. Laser Cut Panel.  
<http://solartran.com.au/lasercutpanel.htm>.
21. SerraGlaze® Daylight Redirecting Film. SerraLux Inc.  
<http://serraluxinc.com/>.
22. P. J. Milner, US Patent No. 6616285 B2 (2003).
23. P. J. Milner, in *Proceedings of the EPIC 2002 Conference, Lyon, France, October 23–26 2002*, p. 661.  
[http://www.aivc.org/sites/default/files/members\\_area/medias/pdf/Conf/2002/106\\_009%20Milner.pdf](http://www.aivc.org/sites/default/files/members_area/medias/pdf/Conf/2002/106_009%20Milner.pdf).
24. A. G. Kostro, M. Geiger, N. Jolissaint, M. A. G. Lazo, J. L. Scartezzini, Y. Leterrier, and A. M. Schuler, *Proc. SPIE* **8485**, 84850L (2012).  
<https://doi.org/10.1117/12.930476>
25. J. Gong, A. Kostro, A. Motamed, and A. Schueler, *Sol. Energy* **139**, 412 (2016).  
<https://doi.org/10.1016/j.solener.2016.10.012>
26. J. Gong, F. D. Meyer, Y. Letterier, A. Kostro, and A. Schueler, *Energy Proc.* **122**, 763 (2017).  
<https://doi.org/10.1016/j.egypro.2017.07.393>
27. J. Gong, A. Delaunay, A. Kostro, and A. Schuler, *Microelectron. Eng.* **191**, 48 (2018).  
<https://doi.org/10.1016/j.mee.2018.01.032>
28. L. J. Hornbeck, *Proc. SPIE* **1150**, 86 (1989).  
<https://doi.org/10.1117/12.962188>
29. M. D. Canonica, F. Zamkotsian, P. Lanzon, W. Noell, and N. D. Rooij, *Opt. Express* **21**, 22400 (2013).  
<https://doi.org/10.1364/OE.21.022400>
30. M. Pizzi, V. Koniachkine, O. de Martiis, and R. Marbach, in *Proceedings of the IEEE/LEOS International Conference on Optical MEMS, 2003*, p. 173.  
<https://doi.org/10.1109/OMEMS.2003.1233521>
31. H. Hillmer, J. Schmid, and I. Stadler, US Patent No. 7677742 B2 (2010).
32. B. Lamontagne and C. Py, US Patent No. 7684105 B2 (2010).
33. K. Mori, K. Misawa, S. Ihida, T. Takahashi, H. Fujita, and H. A. Toshiyoshi, *IEEE Photon. Technol. Lett.* **28**, 593 (2016).  
<https://doi.org/10.1109/LPT.2016.2514299>
34. B. Lamontagne, N. R. Fong, I. H. Song, P. Ma, P. Barrios, and D. Poitras, *J. Micro/Nanolithogr., MEMS MOEMS* **18**, 040900 (2019).  
<https://doi.org/10.1117/1.JMM.18.4.040901>
35. V. Viereck, A. Schwank, and U. Neumann, DBU Final Report No. AZ 23717 (Kassel, 2009).
36. V. Viereck, A. Jäkel, U. Neumann, A. Schwank, H. Hillmer, and J. Schmid, in *Proceedings of the International Solar Energy Society Conference SWC 2011, Kassel, Germany, 2011*.  
<https://doi.org/10.18086/swc.2011.04.09>
37. H. Hillmer, B. Al-Qargholi, M. M. Khan, N. Worapatrakul, H. Wilke, C. Woidt, and A. Tatzel, *Jpn. J. Appl. Phys.* **57**, 08PA07 (2018).  
<https://doi.org/10.7567/JJAP.57.08PA07>
38. N. Worapatrakul, Ph.D. Dissertation (Kassel Univ., 2017).  
<https://doi.org/10.19211/KUP9783737602792>
39. P. D. Floyd and W. A. de Groot, US Patent No. 8724202 B2 (2014).

*Translated by N. Petrov*